

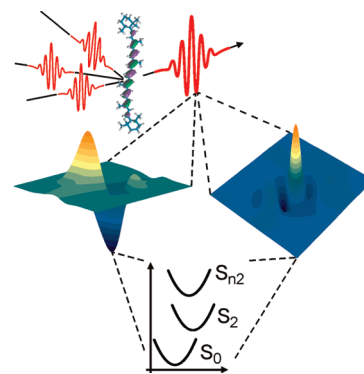
Electronic Double-Quantum Coherences and Their Impact on Ultrafast Spectroscopy: The Example of β -Carotene

Niklas Christensson,[†] Franz Milota,^{†,‡} Alexandra Nemeth,[†] Igor Pugliesi,[‡] Eberhard Riedle,[‡] Jaroslaw Sperling,[†] Tõnu Pullerits,[§] Harald F. Kauffmann,^{†,||} and Jürgen Hauer^{*,†}

[†]Faculty of Physics, University of Vienna, Strudlhofgasse 4, 1090 Vienna, Austria, [‡]Lehrstuhl für BioMolekulare Optik, Ludwig-Maximilians-University, Oettingenstrasse 67, 80538 Munich, Germany, [§]Department of Chemical Physics, Lund University, Box 124, 21000, Lund, Sweden, and ^{||}Faculty of Physics, Vienna University of Technology, Wiedner Hauptstrasse 8 - 10, 1040 Vienna, Austria

ABSTRACT The energy level structure and dynamics of biomolecules are important for understanding their photoinduced function. In particular, the role of carotenoids in light-harvesting is heavily studied, yet not fully understood. The conventional approach to investigate these processes involves analysis of the third-order optical polarization in one spectral dimension. Here, we record two-dimensional correlation spectra for different time-orderings to characterize all components of the transient molecular polarization and the optical signal. Single- and double-quantum two-dimensional experiments provide insight into the energy level structure as well as the ultrafast dynamics of solvated β -carotene. By analysis of the lineshapes, we obtain the transition energy and characterize the potential energy surfaces of the involved states. We obtain direct experimental proof for an excited state absorption transition in the visible ($S_2 \rightarrow S_{n2}$). The signatures of this transition in pump–probe transients are shown to lead to strongly damped oscillations with characteristic pump and probe frequency dependence.

SECTION Kinetics, Spectroscopy



Carotenoids are a family of pigments with important biological functions ranging from dynamic photoprotection and singlet oxygen scavenging to utilization of blue-green light in photosynthesis.¹ The excited-state electronic structure and dynamics of carotenoids are intimately related to their function and have therefore been studied extensively. If a carotenoid is excited with light, the initially prepared excited state S_2 ($1B_u^+$) decays toward the lowest excited, optically dark state S_1 ($2A_g^-$) on a chain length-dependent, sub-200 fs time scale.¹ Several optically dark states have been predicted theoretically and proposed to participate as intermediates in this internal conversion process.² Despite the use of ever shorter pulses in pump–probe experiments,^{3,4} no unified picture of carotenoid's energy deactivation network has emerged yet.^{2,5–8}

A similar situation is found for many molecules of biological and chemical interest. This calls for new experimental techniques disentangling the various contributions to the third-order optical response. One approach is to resolve the induced polarization in excitation frequency. This is achieved in single-quantum two-dimensional spectroscopy (1Q-2D)^{9,10} by correlating coherence evolutions during the first and third time interval of a four-wave mixing sequence. The combination of high spectral and temporal resolution, the capacity of extracting correlation functions, and the reduced spectral

congestion are the key advantages of 1Q-2D over pump–probe. Nevertheless, 1Q-2D still interrogates the same contributions to the third-order optical polarization as pump–probe.

To further refine the understanding of the excited state dynamics, it is therefore desirable to employ methods that probe specific Liouville pathways. In this work we introduce double-quantum two-dimensional spectroscopy (2Q-2D)^{11–14} to selectively probe a state *above* S_2 with an excited state absorption (ESA) transition ($S_2 \rightarrow S_{n2}$) in the visible spectral range. The 2Q-2D experiment singles out Liouville pathways that involve S_{n2} and is insensitive to stimulated emission (SE) and ground-state bleach (GSB). Properly characterizing ESA from S_2 is important for understanding the complex interplay of ultrafast optical responses in carotenoids.^{6,13,14} Previous pump–probe experiments have revealed an ESA transition from S_2 in the near-infrared spectral range.¹⁵ In the visible, such direct assignment is more complicated due to pronounced vibrational wave packet motion,¹⁶ evolving Stokes shift and the overlap of GSB, SE, and the rising ESA from S_1 .

Received Date: October 13, 2010

Accepted Date: November 9, 2010

Published on Web Date: November 15, 2010

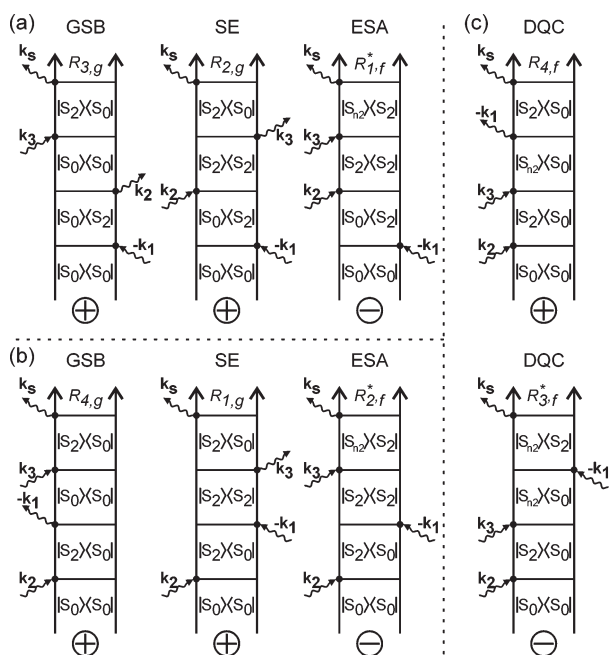


Figure 1. Double-sided Feynman diagrams representing contributions to the third-order optical response of a three-level system S_0 , S_2 , and S_{n2} . The GSB, SE, and ESA are depicted (a) for the rephasing and (b) for the nonrephasing pulse order. (c) DQC pathways.

We measure and discuss a 2Q-2D signal in β -carotene that gives direct experimental proof for an $S_2 \rightarrow S_{n2}$ ESA transition in this spectrally congested region. This contribution directly affects the excited state dynamics of carotenoids and therefore has to be included in the analysis of other third-order optical experiments. By analyzing the line shapes of the 1Q-2D and 2Q-2D spectra, we investigate the potential energy surface (PES) of S_{n2} and the correlation of spectral motions in the different electronic states S_0 , S_2 , and S_{n2} . The employed experimental techniques for the study of higher lying excited states is not specific for carotenoids, and many other systems are expected to benefit from analogous investigations.

1Q-2D and 2Q-2D investigate different components of the third-order polarization and must be discussed on a common footing in order to obtain a comprehensive understanding of the total nonlinear response. The different signal contributions in the $k_S = -k_1 + k_2 + k_3$ phase matching direction for a three-level-system including S_0 , S_2 , and S_{n2} are illustrated by the Feynman diagrams in Figure 1a–c. The wave vector index refers to a given pulse in the experiment and not to the order in which the pulses arrive at the sample. We define t_1 as the delay between the first and the second pulse and t_2 as that between the second and third.¹⁷ t_3 denotes the delay between the third pulse and the signal field.

The ordering of the conjugate field (i.e., $-k_1$) in the pulse sequence defines three different experimental signals: S_I (time order 1–2–3) and S_{II} (2–1–3) correspond to the well-known rephasing and nonrephasing signals. The 1Q-2D spectrum $S^{1Q2D}(\omega_1, t_2, \omega_3)$ at a given t_2 is obtained by Fourier-transformation along t_1 of the signal field emitted during t_3 , and by adding S_I and S_{II} contributions. For the S_{III} signal, three

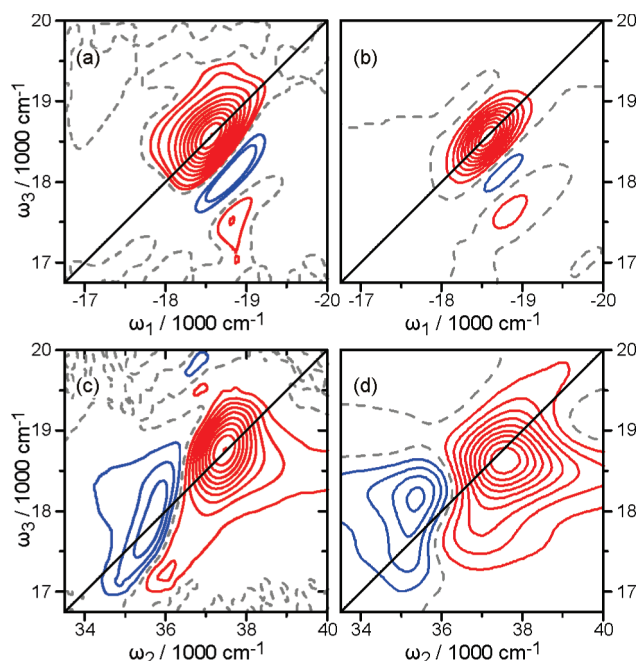


Figure 2. Experimental and simulated 1Q-2D at $t_2 = 0$ fs (a,b) and 2Q-2D spectra at $t_1 = 0$ fs (c,d). Red (blue) lines indicate positive (negative) signals. Lines are drawn with 10% increments, and all spectra are normalized to their respective maximum absolute value. Nodal lines (lines of zero intensity) are dashed.

consecutive energy levels with comparable energy separation are a necessary prerequisite. Double-quantum coherences (DQC) can be induced in such a system if the conjugate field interacts last in the pulse sequence (time order 2–3–1). This time ordering corresponds to negative delays in pump–probe. The Feynman diagrams contributing to S_{III} are depicted in Figure 1c. These pathways, unlike the ones in Figure 1a,b, evolve in a $|S_{n2}\rangle\langle S_0|$ -DQC during t_2 and oscillate at roughly twice the single-quantum coherence frequency. The S_{III} measurement is carried out for a given t_1 by scanning t_2 and detecting the signal field during t_3 . The corresponding 2Q-2D signal $S^{2Q2D}(t_1 = 0, \omega_2, \omega_3)$ is then obtained via a Fourier-transformation over t_2 .

The experimental layout enabling both 1Q- and 2Q-2D measurements in the folded boxcar geometry has been described in detail previously.^{13,18} 1Q-2D and 2Q-2D experiments were carried out using pulses of 1280 cm^{-1} full width at half-maximum (fwhm) bandwidth centered at 18350 cm^{-1} (545 nm). The pulses were compressed to a duration of 16 fs fwhm using a combination of prism compressor and chirped mirrors. Figure 2a shows the real part of the measured 1Q-2D spectrum of β -carotene at $t_2 = 0$ fs, while simulations are shown in Figure 2b. The 1Q-2D spectrum displays a major positive contribution due to GSB and SE located at $\omega_1 = \omega_3 = 18500 \text{ cm}^{-1}$. In addition, there is a smaller positive contribution red-shifted along ω_3 from the GSB. This feature can be identified as the ground-state wave packet of the 1150 cm^{-1} mode based on its energetic position and oscillatory motion during t_2 .¹⁹ One can also observe a negative feature between the two positive contributions. Due to the tilt of the spectrum, this component is almost absent in the projection of the

1Q-2D signal onto ω_3 , i.e. the spectrally resolved pump–probe signal.¹⁰ This negative feature is already an indication of ESA from S_2 . However, it cannot serve as direct proof for the existence of S_{n2} because negative components in the 1Q-2D spectrum can appear already for a two-level system coupled to high-frequency vibrational modes²⁰ or for strong system–bath interaction.²¹

To obtain a signal probing S_{n2} directly, we turn to the 2Q-2D experiment. The measured spectrum shown in Figure 2c (simulations in Figure 2d) was recorded at $t_1 = 0$ fs and reveals two oppositely signed features corresponding to the two Feynman diagrams in Figure 1c. The negative feature is located at lower ω_3 showing that the energy of S_{n2} is less than twice the GSB transition energy. The 2Q-2D spectrum does not display the characteristic antidiagonal elongation as seen for quantum wells^{11,17} or as predicted for 2Q-2D spectra in the homogeneous limit. This implies that the correlated bath motions during different time periods need to be taken into account in the analysis of the experimental results.¹³

On the basis of third-order perturbation theory, we simulate our measurements to extract the additional information in the lineshapes of the 1Q- and 2Q-2D spectra. In the limit of δ -pulse excitation, time ordering defines the contributions to a given experiment as laid out in the discussion of Figure 1. For finite pulses, one must consider the contributions from all orderings and delays of the electric field interactions (t_a , t_b , t_c) permitted by the electric field envelopes. Therefore, an experiment with finite pulses has contributions from Liouville pathways that are not accessible in the impulsive limit. This means that the DQC pathways (Figure 1c) will contribute to the 1Q-2D signal just as single quantum pathways (Figure 1a,b) will affect 2Q-2D spectra during pulse overlap. To accurately account for the pulse overlap effects in the simulations, we used the electric fields obtained from a frequency-resolved optical gating experiment.²²

Our β -carotene model is based on a three-level system coupled to a heat bath. The model employs the second-order cumulant expansion to account for the correlation of bath fluctuations during different time intervals.^{13,19,23} The simulations allow us to determine the properties of the $S_2 \rightarrow S_{n2}$ transition and its coupling to the bath. We used a vertical transition energy of $\omega_{S_{n2}} = 15\,550\text{ cm}^{-1}$. The bath consists of three overdamped modes, $\tau_G = 40\text{ fs}$, $\lambda_G^{S_2} = 90\text{ cm}^{-1}$, $\tau_{E1} = 150\text{ fs}$, $\lambda_{E1}^{S_2} = 180\text{ cm}^{-1}$, and $\tau_{E2} = 150\text{ fs}$, $\lambda_{E2}^{S_2} = 450\text{ cm}^{-1}$, where τ is the characteristic time of the mode, λ is the reorganization energy, and G and E refer to Gaussian and exponential components, respectively. The high frequency vibrational modes are modeled with two under-damped oscillators, $\nu_{v1} = 1520\text{ cm}^{-1}$, $\lambda_{v1}^{S_2} = 960\text{ cm}^{-1}$ and $\nu_{v2} = 1150\text{ cm}^{-1}$, $\lambda_{v2}^{S_2} = 571\text{ cm}^{-1}$. The lifetime of S_2 was set to 150 fs according to the experimental finding. Figure 3 shows a sketch of the PESs for the three levels S_0 , S_2 , and S_{n2} along a generalized coordinate q_j together with definitions of the transitions energies, displacements, and reorganization energies. For the PES of S_{n2} we used significantly smaller displacements of both the overdamped modes, $d_j^{S_{n2}} = \sqrt{0.15}d_j^{S_2}$, and the vibrational modes, $d_{v,j}^{S_{n2}} = \sqrt{0.15}d_{v,j}^{S_2}$. Our results show that the spectral fluctuations of S_{n2} and S_2 are only partially

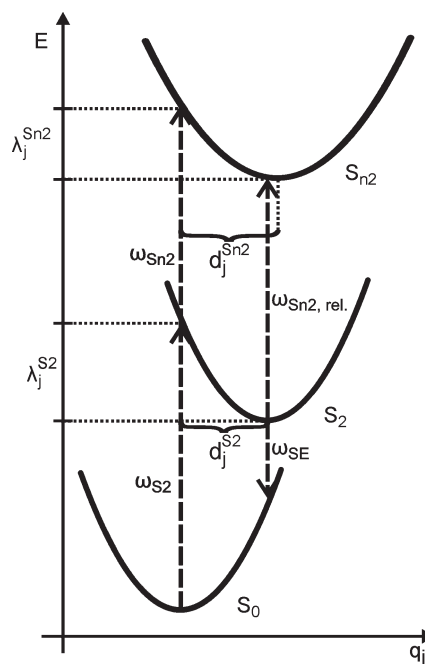


Figure 3. Sketch of PESs for the S_0 , S_2 , and S_{n2} states for a generalized coordinate q_j . The vertical transition energies, dimensionless displacements, and reorganization energies are indicated by ω , d , and λ , respectively. We observe the maximum of the $S_2 \rightarrow S_{n2}$ ESA contribution at $\omega_{S_{n2},rel} \approx 17\,000\text{ cm}^{-1}$, i.e., blue-shifted compared to the vertical transition energy.

correlated, i.e., $0 < d_j^{S_{n2}} \ll d_j^{S_2}$. This is related to the weaker coupling between electronic and nuclear degrees of freedom in S_{n2} .

Whether $S_2 \rightarrow S_{n2}$ makes a significant contribution in optical experiments is determined by its transition dipole moment, $\mu_{S_2 \rightarrow S_{n2}}$. On the basis of combined simulations of the 1Q-2D and the 2Q-2D spectrum in Figure 2, we estimate $\mu_{S_2 \rightarrow S_{n2}}$ to be 0.36 in units of the GSB. The model and parameters discussed above allow for a consistent as well as highly accurate description of the linear absorption spectrum, 1Q-2D, and 2Q-2D experiments.

The $S_2 \rightarrow S_{n2}$ transition characterized in this work has implications for a number of investigations of carotenoid excited-state dynamics. First, it quantifies proposed analogous assignments of such a transition derived with indirect methods.^{5,19,23} Second, it shows that all pathways associated with $S_2 \rightarrow S_{n2}$ need to be considered in the analysis of the ultrafast optical response of carotenoids. To demonstrate this, we show in Figure 4a a pump–probe transient at $\omega_{exc} = 21\,000\text{ cm}^{-1}$ (475 nm) and $\omega_{pr} = 16\,250\text{ cm}^{-1}$ (615 nm). For these calculations, we used 60 fs pump and probe pulses, which are comparable to previous experimental studies.⁸ We partition the signal into its constituents, i.e., SE, $S_2 \rightarrow S_{n2}$ (ESA+DQC), and $S_1 \rightarrow S_{n1}$ (ESA from the relaxed S_1 state). We find that the $S_2 \rightarrow S_{n2}$ signal peaks at $t_2 \approx 20\text{ fs}$, whereas the SE contribution reaches its maximum around $t_2 = 50\text{ fs}$. The $S_1 \rightarrow S_{n1}$ contribution rises comparatively slowly as a result of the finite electronic relaxation from the S_2 state. The total transient displays a modulation that appears like a strongly damped oscillation with an effective period of 120 fs. The differing rise dynamics of the $S_2 \rightarrow S_{n2}$ signal and the SE in

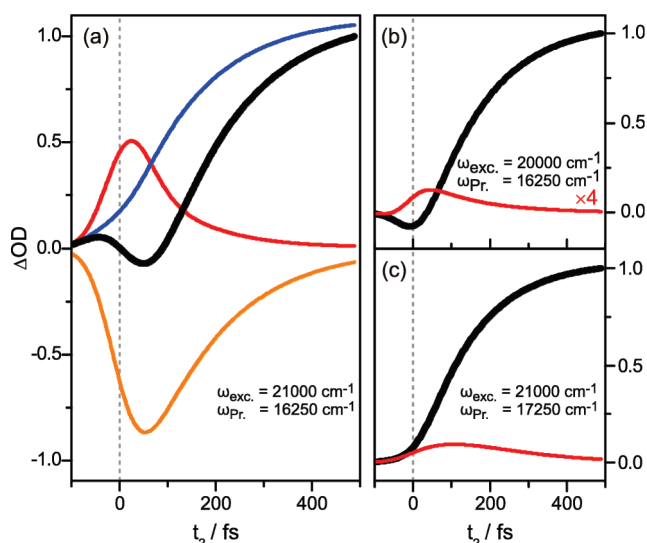


Figure 4. Calculated transient absorption traces for different pump and probe frequencies. (a) $\omega_{\text{exc}} = 21\,000\text{ cm}^{-1}$, $\omega_{\text{pr}} = 16\,250\text{ cm}^{-1}$. The total signal (thick black solid) has been partitioned into SE (orange), $S_2 \rightarrow S_{n2}$ (ESA+DQC) (red), and $S_1 \rightarrow S_{n1}$ (blue) contributions. (b) Pump–probe signal for $\omega_{\text{exc}} = 20\,000\text{ cm}^{-1}$, $\omega_{\text{pr}} = 16\,250\text{ cm}^{-1}$. (c) Pump–probe signal for $\omega_{\text{exc}} = 21\,000\text{ cm}^{-1}$, $\omega_{\text{pr}} = 17\,250\text{ cm}^{-1}$. The thin red lines in panels b and c show the $S_2 \rightarrow S_{n2}$ contribution.

Figure 4a are related to the DQC pathways adding to the former. As shown in Figure 4b,c, we only observe a significant modulation of the transient if we pump close to the first peak of the linear absorption spectrum and probe around $16\,250\text{ cm}^{-1}$. It is only for this combination of pump and probe frequencies that the rise of SE and $S_2 \rightarrow S_{n2}$ are sufficiently different to result in a modulation.

The dependence of the modulation on pump and probe frequency shown in Figure 4 can be understood by considering two different effects. First, changing the pump frequency alters the initial preparation of nuclear modes in S_2 , thereby reshaping the amplitude and shape of the spectra as well as the temporal profiles of the various contributions. Pumping on the red edge leads to faster rise of SE and $S_2 \rightarrow S_{n2}$ ESA as well as a relative decrease in the $S_2 \rightarrow S_{n2}$ ESA amplitude. The second effect concerns the pump and probe frequency dependence of the DQC response functions and can be understood from their oscillations during the second time period, $\exp(i(\Delta_{\text{exc}} + \Delta_{\text{pr}}) \cdot t_b)$.²³ Here, t_b is the actual delay between the second and third electric field interactions, and $\Delta_{\text{exc}} = \omega_{\text{exc}} - \omega_{S_0-S_2}$ and $\Delta_{\text{pr}} = \omega_{\text{pr}} - \omega_{S_2-S_{n2}}$ are detunings defined with respect to the vertical electronic transitions. With the pump tuned to the first peak of the linear absorption spectrum (Figure 4a), the pump and probe detunings partially cancel, and the DQC response functions vary slowly with t_b . On the other hand, pumping at the red (Figure 4b) or blue edge of the linear absorption spectrum gives rise to fast oscillations of the DQC response functions. Such rapidly evolving terms will average out over the finite envelopes of the pulses and make insignificant contributions to the total signal. Similarly, shifting the probe frequency (Figure 4c) leads to diminished DQC contributions and an $S_2 \rightarrow S_{n2}$ signal that is

dominated by the ESA pathways. However, the dependence on probe frequency is more complicated since one also needs to consider the frequency-dependent ratio of DQC to ESA contributions. The observed modulation in the pump–probe transients is readily explained by the DQC pathways inherent to three-level systems. Predicting the specific combination of pump and probe frequencies leading to the highest visibility of the oscillations is a nontrivial problem, making detailed analysis of these features difficult. Therefore, 1Q-2D and 2Q-2D measurements quantifying the different polarization components are the only way to obtain complete information about the system and its dynamics.

Recently, strongly damped oscillations in pump–probe transients were observed in the spectral range from 600 to 700 nm for β -carotene and lutein.⁸ These oscillations were found to depend on both pump and probe frequencies and were only observed if the pump was tuned to the first peak of the linear absorption spectrum. These results were interpreted as quantum beats due to strong electronic coupling between S_2 ($1B_u^+$) and a “dark” state ($1B_u^-$). Such a model also predicts a doubly excited state formed by simultaneous excitation of $1B_u^+$ and $1B_u^-$, leading to extra diagonal and off-diagonal peaks in the 2Q-2D spectrum²⁴ not seen in our experiment. Rather, the 2Q-2D experiment reveals the presence of S_{n2} , implying that all pathways associated with this transition are required for the proper description of the ultrafast response. The inclusion of DQC pathways and finite pulse effects explain the experimentally observed modulations directly, as well as the pump and probe frequency dependence as shown in Figure 4.

Via the use of coherent multidimensional spectroscopy, we dissect the intricate nonlinear optical response of β -carotene in solution. By expanding the signal in higher dimensions and exploiting time ordering to isolate specific signal contributions, we reveal and characterize the hitherto unknown $S_2 \rightarrow S_{n2}$ transition in the visible. Our method lets us derive a model, which (i) is in excellent agreement with 1Q-2D and 2Q-2D measurements, (ii) characterizes spectral motions on the involved PES, (iii) and explains pump-frequency-dependent oscillations in pump–probe transients without invoking “dark” electronic states. Our results clearly demonstrate that electronic states in the vicinity of twice the GSB energy are sparse and display structured features. These states give rise to complicated coherence signatures, which are best analyzed with the combination of 1Q- and 2Q-2D spectroscopy. We expect this approach to be of interest for the studies of molecular aggregates and pigment–protein complexes where two-exciton states give rise to strong ESA signatures.

AUTHOR INFORMATION

Corresponding Author:

*To whom correspondence should be addressed. E-mail: juergen.hauer@univie.ac.at.

ACKNOWLEDGMENT This work has been supported by the Austrian Science Foundation (FWF) within the projects P22331 and F016/18 (ADLIS), the Austrian Academy of Sciences, the Wenner-Gren foundation, the Swedish Research Council, and the Deutsche Forschungsgemeinschaft through the DFG-Cluster of Excellence Munich-Centre for Advanced Photonics.

REFERENCES

- (1) Polivka, T.; Sundström, V. Ultrafast Dynamics of Carotenoid Excited States—From Solution to Natural and Artificial Systems. *Chem. Rev.* **2004**, *104*, 2021–2071.
- (2) Polivka, T.; Sundström, V. Dark Excited States of Carotenoids: Consensus and Controversy. *Chem. Phys. Lett.* **2009**, *477*, 1–11.
- (3) Cerullo, G.; Polli, D.; Lanzani, G.; De Silvestri, S.; Hashimoto, H.; Cogdell, R. J. Photosynthetic Light Harvesting by Carotenoids: Detection of an Intermediate Excited State. *Science* **2002**, *298*, 2395–2398.
- (4) Polli, D.; Cerullo, G.; Lanzani, G.; De Silvestri, S.; Yanagi, K.; Hashimoto, H.; Cogdell, R. J. Conjugation Length Dependence of Internal Conversion in Carotenoids: Role of the Intermediate State. *Phys. Rev. Lett.* **2004**, *93*, 163002.
- (5) Papagiannakis, E.; van Stokkum, I. H. M.; Vengris, M.; Cogdell, R. J.; van Grondelle, R.; Larsen, D. S. Excited-State Dynamics of Carotenoids in Light-Harvesting Complexes. 1. Exploring the Relationship between S1 and S* States. *J. Phys. Chem. B* **2006**, *110*, 5727–5736.
- (6) Kosumi, D.; Komukai, M.; Hashimoto, H.; Yoshizawa, M. Ultrafast Dynamics of All-*trans*- β -Carotene Explored by Resonant and Nonresonant Photoexcitations. *Phys. Rev. Lett.* **2005**, *95*, 213601.
- (7) Lustres, J. L. P.; Dobryakov, A. L.; Holzwarth, A.; Veiga, M. S2–S1 Internal Conversion in β -Carotene: Strong Vibronic Coupling from Amplitude Oscillations of Transient Absorption Bands. *Angew. Chem., Int. Ed.* **2007**, *46*, 3758–3761.
- (8) Ostroumov, E.; Muller, M. G.; Marian, C. M.; Kleinschmidt, M.; Holzwarth, A. R. Electronic Coherence Provides a Direct Proof for Energy-Level Crossing in Photoexcited Lutein and β -Carotene. *Phys. Rev. Lett.* **2009**, *103*, 108302.
- (9) Cho, M. H. Coherent Two-Dimensional Optical Spectroscopy. *Chem. Rev.* **2008**, *108*, 1331–1418.
- (10) Jonas, D. M. Two-Dimensional Femtosecond Spectroscopy. *Annu. Rev. Phys. Chem.* **2003**, *54*, 425–463.
- (11) Stone, K. W.; Gundogdu, K.; Turner, D. B.; Li, X. Q.; Cundiff, S. T.; Nelson, K. A. Two-Quantum 2D FT Electronic Spectroscopy of Biexcitons in GaAs Quantum Wells. *Science* **2009**, *324*, 1169–1173.
- (12) Kim, J.; Mukamel, S.; Scholes, G. D. Two-Dimensional Electronic Double-Quantum Coherence Spectroscopy. *Acc. Chem. Res.* **2009**, *42*, 1375–1384.
- (13) Nemeth, A.; Milota, F.; Mancal, T.; Pullerits, T.; Sperling, J.; Hauer, J.; Kauffmann, H. F.; Christensson, N. Double-Quantum Two-Dimensional Electronic Spectroscopy of a Three-Level System: Experiments and Simulations. *J. Chem. Phys.* **2010**, *133*, 094505.
- (14) Mukamel, S.; Oszwaldowski, R.; Yang, L. A Coherent Nonlinear Optical Signal Induced by Electron Correlations. *J. Chem. Phys.* **2007**, *127*, 221105.
- (15) Zhang, J. P.; Skibsted, L. H.; Fujii, R.; Koyama, Y. Transient Absorption from the 1B(u)(+) State of All-*trans*- β -Carotene Newly Identified in the Near-Infrared Region. *Photochem. Photobiol.* **2001**, *73*, 219–222.
- (16) Hauer, J.; Buckup, T.; Motzkus, M. Pump-Degenerate Four Wave Mixing as a Technique for Analyzing Structural and Electronic Evolution: Multidimensional Time-Resolved Dynamics Near a Conical Intersection. *J. Phys. Chem. A* **2007**, *111*, 10517–10529.
- (17) Karaiskaj, D.; Bristow, A. D.; Yang, L. J.; Dai, X. C.; Mirin, R. P.; Mukamel, S.; Cundiff, S. T. Two-Quantum Many-Body Coherences in Two-Dimensional Fourier-Transform Spectra of Exciton Resonances in Semiconductor Quantum Wells. *Phys. Rev. Lett.* **2010**, *104*, 117401.
- (18) Nemeth, A.; Sperling, J.; Hauer, J.; Kauffmann, H. F.; Milota, F. Compact Phase-Stable Design for Single- and Double-Quantum Two-Dimensional Electronic Spectroscopy. *Opt. Lett.* **2009**, *34*, 3301–3303.
- (19) Christensson, N.; Milota, F.; Nemeth, A.; Sperling, J.; Kauffmann, H. F.; Pullerits, T.; Hauer, J. Two-Dimensional Electronic Spectroscopy of β -Carotene. *J. Phys. Chem. B* **2009**, *113*, 16409–16419.
- (20) Mancal, T.; Nemeth, A.; Milota, F.; Lukes, V.; Kauffmann, H. F.; Sperling, J. Vibrational Wave Packet Induced Oscillations in Two-Dimensional Electronic Spectra. II. Theory. *J. Chem. Phys.* **2010**, *132*, 184515.
- (21) Hybl, J. D.; Christophe, Y.; Jonas, D. M. Peak Shapes in Femtosecond 2D Correlation Spectroscopy. *Chem. Phys.* **2001**, *266*, 295–309.
- (22) Christensson, N.; Avlasevich, Y.; Yartsev, A.; Mullen, K.; Pascher, T.; Pullerits, T. Weakly Chirped Pulses in Frequency Resolved Coherent Spectroscopy. *J. Chem. Phys.* **2010**, *132*, 174508.
- (23) Christensson, N.; Polivka, T.; Yartsev, A.; Pullerits, T. Photon Echo Spectroscopy Reveals Structure-Dynamics Relationships in Carotenoids. *Phys. Rev. B* **2009**, *79*, 245118.
- (24) Fulmer, E. C.; Mukherjee, P.; Krummel, A. T.; Zanni, M. T. A Pulse Sequence for Directly Measuring the Anharmonicities of Coupled Vibrations: Two-Quantum Two-Dimensional Infrared Spectroscopy. *J. Chem. Phys.* **2004**, *120*, 8067.